



pubs.acs.org/JPCB Article

Investigation of a Series of 2-(2'-Hydroxyaryl)benzazole Derivatives: Photophysical Properties, Excited-State Intramolecular Proton-Transfer Reactions, and Observation of Long-Lived Triplet Excited States

Published as part of The Journal of Physical Chemistry virtual special issue "125 Years of The Journal of Physical Chemistry".

Yuanchun Li, Xueqin Bai, Runhui Liang, Xiting Zhang, Yen H. Nguyen, Brett VanVeller, Lili Du,* and David Lee Phillips*



Cite This: J. Phys. Chem. B 2021, 125, 12981–12989



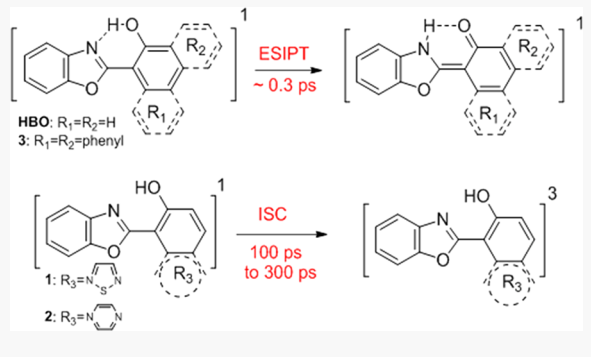
ACCESS

Metrics & More

Article Recommendations

s Supporting Information

ABSTRACT: Excited state intramolecular proton transfer (ESIPT) has drawn much attention for its important applications in a variety of areas. Here, the steady-state and time-resolved absorption spectroscopic experiments as well as DFT/TD-DFT calculations are employed to study the photophysical properties and photochemical reaction mechanisms of 2-(2'-hydroxyphenyl) benzoxazole (HBO) and selected derivatives (compounds 1–3). Because of their larger π -conjugation framework, compounds 1–3 display red-shifted absorbance but blue-shifted fluorescence compared with HBO. A fast ESIPT process is observed directly for HBO while compound 3 has an enol/keto equilibrium type of ESIPT that exhibits dual emission. Interestingly, only the emission of the enol form is observed for compounds 1 and 2



which suggests that the ESIPT process is strongly inhibited. These results indicate the decoration with electron-withdrawing groups such as thiadiazol and pyrazine on the hydroxyphenyl ring (compounds 1 and 2) apparently suppresses the proton-transfer processes in their excited states. Whereas the ESIPT process is rarely increased for compound 3 that modified with the phenanthrol ring, because the effective conjugation is reduced for compound 3 compared with HBO. The work here provides fundamental insights that may be useful for designing novel ESIPT molecules in the future.

INTRODUCTION

Proton-transfer reactions have received considerable attention, because they are fundamental processes in chemistry and biology. 1,2 A number of compounds with intramolecular hydrogen-bonded organic chromophores such as salicylates, oxazoles, and flavones can undergo photoinduced proton transfer to give the corresponding tautomers through an internal hydrogen bond in a subpicosecond time scale, 1,3-5 which is known as excited-state intramolecular proton transfer (ESIPT).^{6–8} A structural prerequisite for the ESIPT process is the presence of an intramolecular H-bond between the proton donor (typically hydroxyl or amino groups) and a proton acceptor (such as a carbonyl oxygen or a nitrogen atom in a heterocycle) nearby. Some well-known ESIPT molecules are salicylic acid (the first reported ESIPT molecule), 10 2-(2hydroxyphenyl) benzothiazole (HBT), and 2-(2-hydroxyphenyl) benzoxazole (HBO). Taking HBO as an example, the basic photophysical processes of the ESIPT chromophores are illustrated in Scheme 1.

ESIPT is a simple chemical process but has attracted much attention because ESIPT-possessing molecules have important applications in a variety of areas, including functional materials, 11,12 fluorescence imaging, 13 UV-photostabilizers, 14,15 solar energy conversion, 16 laser dyes, 17 molecular switches, 18 long-lived pH jumps, 19 and so forth. Despite the unique character and potential practical uses of such compounds, relatively little is known about the structure—property relationships of the reported ESIPT molecules. In addition, the insights into the factors that govern the isomerization and wavelength of emission are immensely valuable to the design of novel molecules that possess ESIPT properties. To address the

Received: July 2, 2021 Revised: October 13, 2021 Published: November 19, 2021





Scheme 1. Molecular Structures of HBO and Its Possible Conformations^a

^aThe numbering in black, blue, red, and green are for carbon, nitrogen, oxygen, and hydrogen atoms, respectively (top). Molecular structures of compounds 1–3 (bottom).

above challenges, we prepared a series of compounds 1-3(Scheme 1) with HBO as the parent molecule due to its chemical stability, structural simplicity, and facility for chemical modification.²⁰ For comparison, the corresponding analogue of HBO and compounds 1-3 without ESIPT character by substituting a methoxy group for the hydroxyl group (Me1-Me3) were prepared and discussed as well. From a fundamental viewpoint, one of the intrinsic factors to adjust the ESIPT parameters lies in the H-bond strength in terms of its distance and/or angle. In this regard, a great number of studies focused on fine-tuning of the H-bond via chemical modification on the parent molecule with a variety of simple electron-withdrawing (e.g., -CF₃, -CN, and acetyl group) or electron-donating groups (such as alkyl) at different positions. 21-24 Another modification strategy is the elongation of the π -conjugated framework, which leads to a red-shifted absorption, 25 and may further expand its application to biomolecular sensing and so on. However, a design on the basis of the judicious balance between both π -elongation and the stabilization of aromaticity is rare.

Herein, the photophysical properties of the titled compounds were studied by steady-state absorption and fluorescence spectra as well as time-resolved transient absorption spectra. The influence of the chemical structure on the photophysical properties was studied with the combination of experimental spectra and theoretical calculations as well. HBO, the parent molecule, is used as a prototype and reference for the study of compounds 1–3. To the best of our knowledge, this is the first time for a report of relationship between structure and ESIPT photophysical properties of HBO derivates, which is of significant importance in the design methodologies of novel ESIPT molecules.

RESULTS AND DISCUSSION

Steady-State Absorption and Emission Spectra. The UV-vis spectra and steady-state emission spectra for HBO and compounds 1-3 in dichloromethane (DCM) are shown in Figures S1-S4, and pertinent data are presented in Table 1. These compounds show sparse solubility in nonpolar solvents, which makes the further femtosecond and nanosecond timeresolved transient absorption measurements infeasible. In some solvents with good solubility such as MeOH, the external Hbond formed between ESIPT molecules and the solvent may drastically suppress ESIPT.1 Therefore, DCM was chosen as the solvent throughout the spectroscopic studies unless otherwise specified. HBO and compounds 1-3 have similar electronic absorption features in DCM, consisting of some intense bands maximized in the UV range (Figures S1-S4) with a molar absorptivity (ε) ranging from 1157 to 25 095 M⁻¹ cm⁻¹, which are mainly ascribed to the typical $\pi - \pi^*$ transitions of the conjugated backbone of these molecules. However, it is worth mentioning that the absorption maximums of compounds 1-3 show a remarkable red-shift compared with HBO because of the decrease of the energy gap between the HOMO and LUMO via an extension of the π conjugation framework. For compounds Me1-Me3, the alkylation of the hydroxyl moiety makes the UV-vis absorption spectra blue-shifted due to the absence of an intramolecular hydrogen bond.²⁶

Although there are great similarities among the absorption spectra of the four compounds, their emission spectra are very different. Through analysis of the Stokes shift and comparison of the emission spectra between the target molecules and the corresponding methylated molecules, whether ESIPT is inhibited can be revealed directly and visually. **HBO** shows dual emissions with a large Stokes shift emission (>9322 cm $^{-1}$) of keto (S₁) generated from the enol (S₁) via an ESIPT process. ^{30,31} Enol (S₁) emission at 364 nm is favored in protic solvent (MeOH), and keto (S₁) has the predominant emission in nonpolar solvent. Different from **HBO**, the emission bands of compound **1** show a single band irrespective of the solvent

Table 1. Observed Steady-State Absorption/Emission Band Maximum (λ /nm), Molar Absorptivity (ϵ), and Stokes Shift as Well as the Enol/Keto Fluorescence Area Ratio^{27–29} of Compounds HBO and 1–3^a

compound	observed $\lambda_{ m abs}/ m nm \ (arepsilon/ m M^{-1}\ cm^{-1})$	computed $\lambda_{\rm abs}/{\rm nm}$ (f)	observed $\lambda_{ m em}/{ m nm}$ enol/keto	enol/keto fluorescence area ratio b	observed Stokes shift enol/keto (cm ⁻¹)
НВО	334 (16518)	325 (0.66)	364:485	1:29	2468:9322
3	380 (25095)	361 (0.73)	405:439	1:2.5	1624:3537
2	363 (6184)	358 (0.45)	431, 452 ^c	1:0	4346, 5424
1	374 (1157)	375 (0.40)	462 ^c	1:0	5093

"Compounds obtained in DCM at room temperature. Computed absorption wavelengths and oscillator strengths (f) of the first singlet excitation in the enol form are also listed in the table. Theoretical calculations were performed at wB97XD/def2tzvp (DCM) level of theory. Quantitative resolution of the emission spectra was done with mathematical analysis with the assumption that enol (S_1) and keto (S_1) have individual areas of emission for **HBO** and compound 3. Integration of the individual fluorescence area was employed to determine the enol/keto fluorescence area ratio. Conly the emissions of enol are observed for compounds 1 and 2.

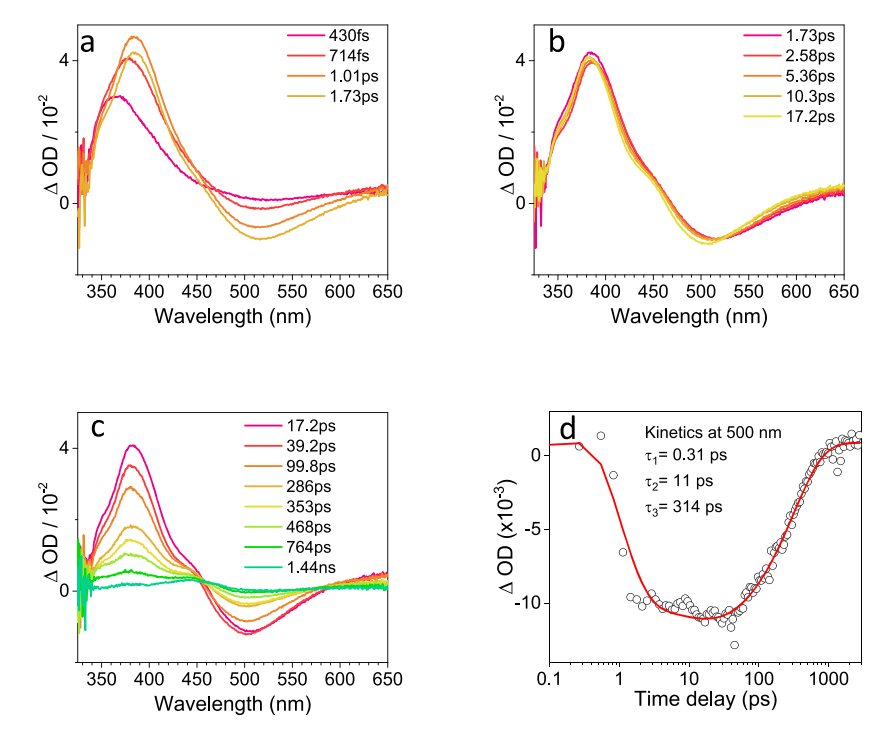


Figure 1. (a-c) Fs-TA spectra of HBO in DCM upon 267 nm photoexcitation and (d) the kinetics of the characteristic transient absorption band observed at 500 nm. The solid line indicates the fitting to the experimental data.

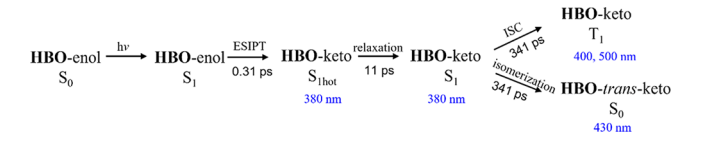
as shown in Figure S2b, indicating the prohibition of ESIPT. Furthermore, similar single-emission profiles are found for compound Me1 in different solvents. Thus, it is reasonable to assume that compound 1 does not undergo ESIPT upon photoexcitation, which may be due to the weak aromaticity and strong electronegativity. The absence of ESIPT for compound 1 also supports that the ESIPT can be eliminated by π -conjugation variations.³² Next, we replaced the thiadiazole segment of compound 1 with quinoxalinol which led to the formation of compound 2. As shown in Figure S3b for compound 2, the emission profiles show a single emission for all solvents except DCM in which the emission of compound 2 has two bands with maxima at 431 and 452 nm with very small separation. If the band 452 nm is assigned to the keto (S₁) form, it usually decreases in a protic solvent. such as MeOH. However, as shown in Figure S3b, the intensity of the band at 452 nm does not change much, but red shifts in MeOH. Thus, we might not be able to assign this band to the keto (S_1) form. Most likely, both bands at 430 and 452 nm are due to the enol (S_1) . The near mirror image relationship between the absorption and emission spectra of compound Me2 in Figure S3a is consistent with the absence of an ESIPTmediated relaxation in the excited state. The absence of the keto fluorescence in compounds 1 and 2 implies there is a significant influence of the electron-withdrawing group on the ESIPT properties. Unlike compounds 1 and 2, two emission bands at 405 nm (shoulder) and 439 nm are observed for compound 3 in DCM. In protic solvents (MeOH), the intensity of the 405 nm emission band increases in comparison to the 439 nm band, which can be attributed to the increased population of solvated-enol. Because the intermolecular hydrogen bonding between compound 3 and the protic solvent competes with the intramolecular hydrogen bond and consequently increases its enol fluorescence intensity in the emission spectrum. Thus, thisome provides a solid piece of evidence that compound 3 will undergo ESIPT upon excitation

and the shoulder band located around 405 nm is due to the radiative decay of enol (S_1) while the long-wavelength emission (439 nm) is from keto (S_1) . Furthermore, the different emission profiles of compounds Me3 and 3 provide further support for these assignments for compound 3.

Time-Resolved Transient Absorption Spectroscopy. To elucidate the reaction mechanism and gain direct information about the reactive intermediates involved, femto-second time-resolved transient absorption spectroscopy (fs-TA) and nanosecond time-resolved transient absorption spectroscopy (ns-TA) experiments were conducted for the four molecules of interest, which provide new insight into the excited-state deactivation dynamics after ESIPT. Furthermore, as a control experiment the fs-TA and ns-TA spectra of the methylated analogues Me1–Me3 were investigated, too. Because of the lack of a hydroxyl proton, ESIPT will not occur for Me1–Me3.

Figure 1a-c displays the time-resolved transient absorption spectra obtained after photolysis of HBO in DCM. Spectra are given separately to clarify the spectral changes that take place in different time scales. After photoexcitation, the transient absorption appears around 365 nm and the broad stimulated emission (SE) band at 510 nm emerges (Figure 1a). From 430 fs to 1.73 ps, the absorption band gradually increases and red shifts to 380 nm, while the SE band grows simultaneously. According to a previous study,³³ the SE band is attributed to the keto (S₁) after the ESIPT process. Therefore, the TA spectral changes in Figure 1a can be assigned to the ESIPT process and the initial species that appears at 365 nm at 0.43 ps can be assigned to the $S_1 \rightarrow S_n$ absorption from enol (S_1) . As displayed in Figure 1b, the temporal spectral evolution at the time delays from 1.73 to 17.2 ps exhibiting an ultrafast timedependent Stokes shift emission of the keto (S_1) may result from the solvent-coupled excited state relaxation. In the later delay times (Figure 1c), the transient absorption at 380 nm decays monotonically with the growth of another absorption band with its maximum at 435 nm (Figure 1c). Such a precursor-successor type of relationship suggests the appearance of a new transient species (denoted as HBO-X₄₃₅) amid the excited state relaxation. The kinetics fitting at 500 nm provides three time constants (Figure 1d): 0.31, 11, and 314 ps, which are assigned to the ESIPT process, the solvent relaxation, and the generation of HBO-X435, respectively. To gain insight into the nature of HBO-X435 and obtain complementary support for the decay dynamics of this new species, we further performed ns-TA experiments for HBO under different solution conditions. These results are shown in Figure S6a and clearly reveal that HBO in DCM exhibits a strong absorption band with a maximum at 435 nm. However, the absorption band at 435 nm is not observed in MeOH, which suggests that HBO- X_{435} can be quenched by a protic solvent. According to previous observations, ^{34–37} especially the proton-catalyzed trans-keto re-enolization, led us to designate the species HBO- X_{435} as the trans-keto (S_0) of HBO, which is consistent with the results reported in a previous work.³⁸ Further support for this assignment comes from results from DFT calculations (Figure S6c), showing that the simulated absorption spectra of trans-keto (S₀) exhibited reasonable similarity with the corresponding experimental spectra. However, the two weak absorption bands centered at 400 and 500 nm detected in MeOH are mainly assigned to the **HBO** triplet states of keto (T_1) , which can be quenched by oxygen.³⁸ Thus, the mechanism of HBO after irradiation can be described as follows (Scheme 2): after ultrafast ESIPT, keto

Scheme 2. Proposed Photophysical and Photochemical Pathways of HBO



 (S_1) is generated from the enol (S_1) . During the process of keto (S_1) 's attenuation, the *trans*-keto and keto (T_1) are produced through isomerization and intersystem crossing (ISC), respectively.

As discussed above, compound 1 is found to be an ESIPT strongly inhibited molecule. As expected, no proton transfer process is observed in DCM by fs-TA as shown in Figure 2. Upon irradiation (Figure 2a), the initial species that emerges with bands at 425 and 580 nm can be assigned to enol (S_1) of compound 1. Later, the band at 580 nm blue shifts from 580 to 572 nm with the intensity increasing, while the band at 425 nm remains almost unchanged (Figure 2b). This spectral variation is tentatively attributed to the solvent-coupled excited state relaxation. After 26.3 ps, the absorbance band at 572 nm gradually red shifts to 610 nm while the absorbance at 425 nm decreases in intensity significantly (Figure 2c), which implies a transformation from enol (S₁) into another transient species (denoted as $1-X_{610}$). Kinetics study at 425 nm of compound 1, as shown in Figure 2d, reveals three time constants: 0.36 ps, 104 ps, and >3 ns, which correspond to the generation of the enol (S_1) , the ISC process and the lifetime of the enol (T_1) species, respectively. For delay times beyond 3 ns, the initial spectrum obtained from ns-TA (Figure S7a) clearly reveals that 1-X₆₁₀ decays slowly without a new species appearing over the delay times examined. The kinetics at 610 nm under open air and argon-saturated conditions were performed (Figure S7c). Remarkable quenching of the TA signals by oxygen suggests that 1-X₆₁₀ is a triplet species. As no ESIPT occurs, 1- X_{610} is reasonably assigned as enol (T_1) , and this is supported by the resemblance of the TD-DFT calculated absorption spectrum of enol (T_1) . The photophysical processes for compound 1 are summarized in Scheme 3. When the hydroxyl group is replaced with the methyl moiety, as shown in Figure S8, the fs-TA and ns-TA spectral profiles of compound Me1 obtained in DCM displayed similarity with that of compound 1. Thus, the electron withdrawing thiadiazole group might

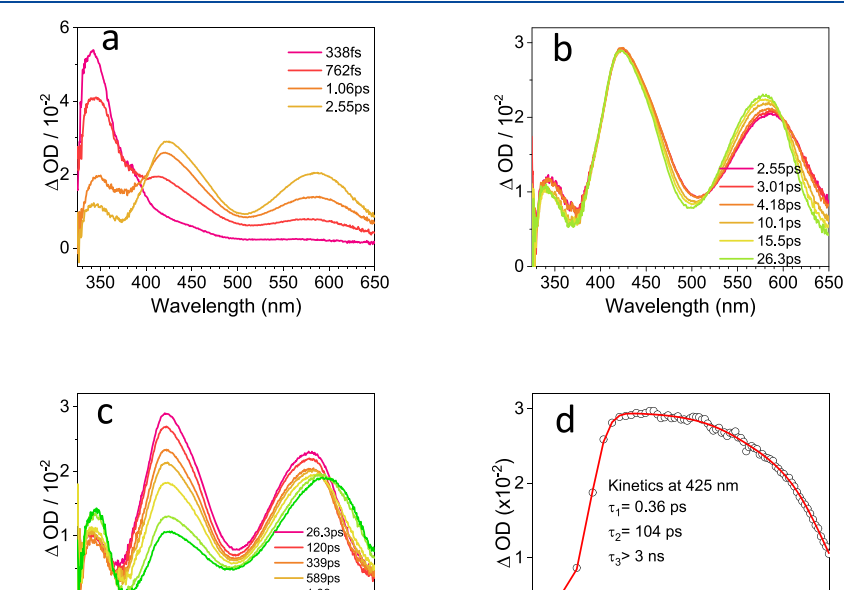


Figure 2. (a-c) Fs-TA spectra of compound 1 in DCM upon 267 nm photoexcitation and (d) the kinetics of the characteristic transient absorption band observed at 425 nm. The solid line indicates the fitting to the experimental data.

0

10

Time delay (ps)

100

1000

2.18ns

350 400 450 500 550 600

Wavelength (nm)

Scheme 3. Proposed Photophysical Pathways of Compound

1-enol
$$\xrightarrow{h\nu}$$
 1-enol $\xrightarrow{0.36}$ ps $\xrightarrow{S_1}$ 1-enol $\xrightarrow{15C}$ 1-enol $\xrightarrow{S_0}$ 1 -enol $\xrightarrow{104}$ ps $\xrightarrow{T_1}$ 425, 580 nm 425, 610 nm

strongly inhibit the migration of the proton on the hydroxyl group, which results in the non-ESIPT processes observed experimentally.

Comparing to thiadiazole, the quinoxalinol group of compound 2 shows less electronegativity, and it has different photophysical properties compared to compound 1 to drive us to investigate it as well. The fs-TA results of compound 2 are displayed in Figure S9 and Figure 3. Upon excitation, compound 2 reveals two transient absorption bands at 407 and 530 nm in the early delay times (Figure S9), which can be assigned to the enol (S_1) of compound 2. At later delay times (Figure 3a), the enol (S_1) decays with absorbance features at 407 and 530 nm diminishing in intensity. Then, both bands at 407 and 530 nm decay significantly with the increasing intensity of a broad new band at 630 nm. The obvious isosbestic point at 560 nm suggests the dynamical conversion between two species. Thus, the new species (named as 2-X₆₃₀) is generated via a transformation from enol (S_1) . In a word, the initial photophysical and photochemical processes of compound 2 in DCM can be summarized as enol $(S_n) \rightarrow \text{enol } (S_1)$ \rightarrow 2-X₆₃₀. Apparently, 2-X₆₃₀ is a long-lived species as shown in Figure 3c. To further resolve this unknown long-lived species 2-X₆₃₀, ns-TA spectra were obtained in Figure S9. It is observed that 2-X₆₃₀ have two comparable characteristic absorptions features at both 400 and 630 nm (Figure S10a) and they decay continuously without transformation into other species. The ns-TA spectra of compound 2 in MeOH (Figure S10b) is similar to that in DCM, indicating 2-X₆₃₀ is not quenched by protic solvents and thus it cannot be assigned to trans-keto (S_0) of compound 2. Whereas in the presence of oxygen in solution, this species has a reduced lifetime (Figure S10c), suggesting 2- X_{630} is a triplet excited state species in nature. Thus, 2- X_{630} can be assigned to enol (T_1). TD-DFT computational results provide further support for this assignment. As displayed in Figure S10d, the corresponding ns-TA spectrum shows reasonable similarity with the calculated absorption spectrum of enol (T_1) but exhibits great differences from the calculated spectrum of keto (T_1). The kinetics fitting of fs-TA data at 620 nm provides three time constants (Figure 3d): 0.42, 26.8 and 275 ps, which are assigned to the IC process from enol (S_n) to enol (S_1), the solvent relaxation and the ISC process, respectively.

The fs-TA of compound Me2 is also displayed in Figure S11 as a reference. Upon irradiation at 267 nm, the ISC process from Me2 (S_1) to Me2 (T_1) is observed with similar absorption patterns as compound 2, which provides supplementary evidence for the assignments of the corresponding species appearing in the TA spectra of compound 2. The reaction mechanism of compound 2 is depicted in (Scheme 4).

Scheme 4. Proposed Photophysical and Photochemical Pathways of Compound 2

When the electron withdrawing group quinoxalinol in compound $\mathbf{2}$ is replaced with phenanthrol, it leads to the formation of compound $\mathbf{3}$. Figure 4 depicts the fs-TA results obtained for compound $\mathbf{3}$ in DCM. At early delay times (Figure 4a), the negative signal within 340-380 nm is contributed by ground state bleaching. Besides, a weak SE band at 486 nm shows up continuously which is due to emission from compound $\mathbf{3}$ keto (\mathbf{S}_1) in DCM. Therefore, the ESIPT process takes place at initial delay times. In the later delay times (Figure 4b) with the dramatic decay of 430 nm, a

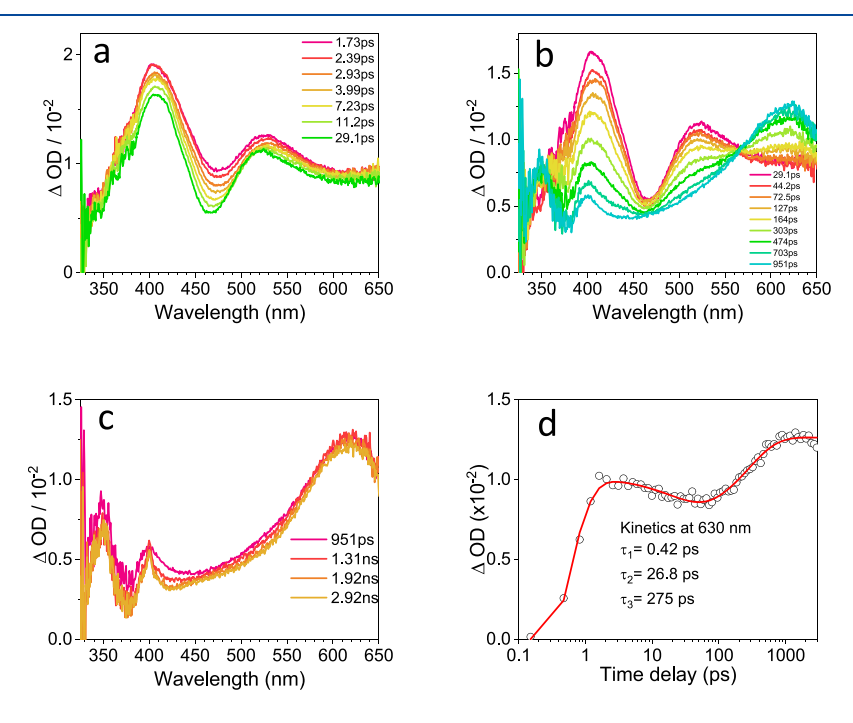


Figure 3. (a-c) Fs-TA spectra of compound 2 in DCM upon 267 nm photoexcitation and (d) the kinetics of the characteristic transient absorption band observed at 630 nm. The solid line indicates the fitting to the experimental data.

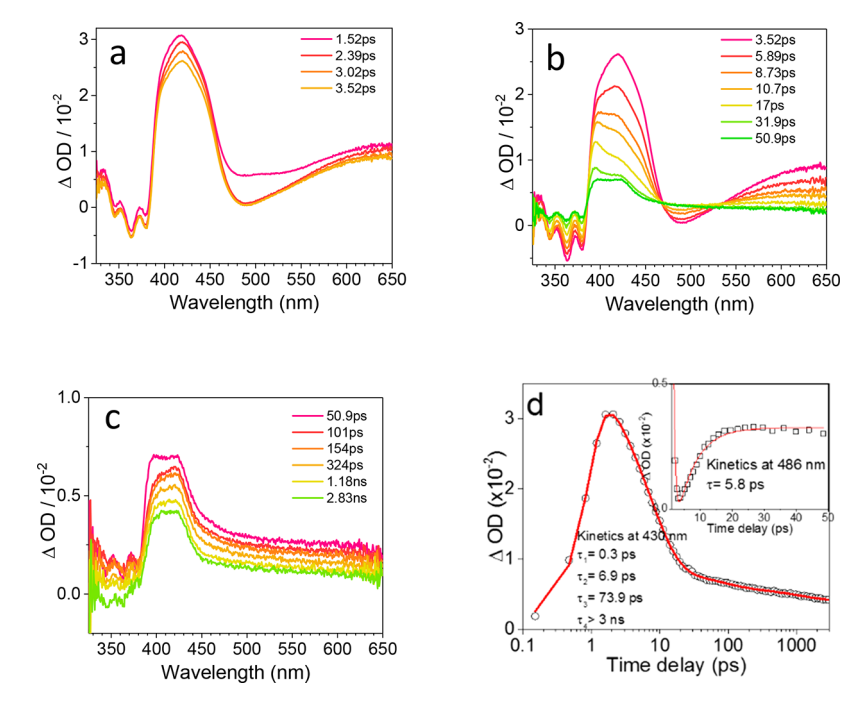
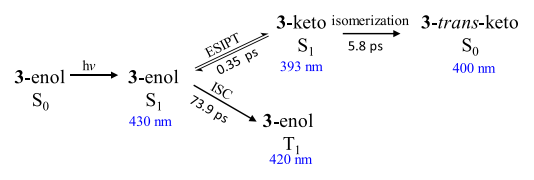


Figure 4. (a-c) Fs-TA spectra of compound 3 in DCM upon 267 nm photoexcitation and (d) the kinetics of the characteristic transient absorption band observed at 430 nm (inserted, 486 nm). The solid line indicates the fitting to the experimental data.

sharp band at 393 nm and another band at 420 nm show up with different decay rates, which suggests two transient species are involved in the process (named as 3-X₃₉₃ and 3-X₄₂₀, individually). Coincidently, the 3-X₃₉₃ disappears at the similar delay time with the SE band and gives birth to the new band at 400 nm (Figure 4c). The kinetics of the SE band monitored at 486 nm can be deconvoluted by a single exponential decay with the time constant 5.8 ps (Figure 4d, inset graph). Thus, we can conclude that 3-X₃₉₃ could also be assigned to the keto (S_1) , whose lifetime is 5.8 ps. With the decay of 3- X_{393} , the new species with a transient absorption band at 400 nm $(3-X_{400})$ is generated, which may be assigned to the trans-keto (S₀) species. Therefore, the initial transient absorption band at 430 nm may be due to the enol (S_1) and the 3- X_{420} can be assigned to the enol (T1) after an ISC process occurs. The kinetics at 430 nm (Figure 4d) can be fitted with four time constants: 0.3 ps, 6.9 ps (5.8 ps), 73.9 ps, and >3 ns. As we discussed above, the ketol (S₁) is generated at early times, thus the 0.3 ps kinetics can be due to the fast ESIPT process. The 6.9 ps (5.8 ps) is due to the IC process from the keto (S1) to the transketo (S_0) . Since 3- X_{420} is produced in the later delay times, we might assign the 73.9 ps to the ISC process. Further quenching experiments in Figure S12 show that this long-lived species is sensitive to protic solvents such as MeOH (Figure S12b) (Figure S12c), which implies 3-X₄₀₀ could be the trans-keto (S_0) species and 3- X_{420} is the enol (T_1) species. The excellent correlation between the calculated trans-keto (S₀) species and transient absorption spectrum at 5 ns shown in Figure S12d provides further support for this assignment.

As a control experiment, the fs-TA of compound **Me3** in DCM was investigated (Figure S13), which experienced a very simple photophysical process after photolysis ($S_0 \rightarrow S_n \rightarrow S_1 \rightarrow S_0$) and did not participate in any photochemical reactions. In summary, the proposed photophysical and photochemical pathways of compound 3 are shown in Scheme 5. Although the ESIPT process is observed for 3, the extension of the π -

Scheme 5. Proposed Photophysical and Photochemical Pathways of Compound 3



conjugation system neither increases the quantum yield of the 3-keto (S_1) species, nor red shifts the emission of 3-keto (S_1) .

DFT/TD-DFT Calculations. To understand the relationship between the molecular structures and the ESIPT properties of these compounds, we carried out theoretical calculations for HBO and compounds 1-3 with DFT and TD-DFT methods. As shown in Figure S14, the potential energy profiles for the singlet-excited states of HBO and compounds 1-3 are displayed. For HBO, upon excitation the hydroxyl proton undergoes an ultrafast transfer to the acceptor N atom after overcoming a small energy barrier of 0.7 kcal/mol, generating keto (S₁) with a much smaller energy ($\Delta E = -5.9$ kcal/mol). Such a large free energy decrease for the transformation indicates a strong driving force for the proton transfer, which coincides with the observed ultrafast ESIPT of HBO. For compound 3, the energy barrier is also small (0.9 kcal/mol), but the energy difference between the enol (S_1) and keto (S_1) barriers is not as significant as that of **HBO**. Such an energy profile feature implies that the ESIPT for compound 3 is ultrafast, but there exists an equilibrium between enol (S_1) and keto (S₁), which leads to the relatively low yield of keto (S_1) and dual emission can be observed. For compound 2, the energy gap climbs to 1.5 kcal/mol, which is larger than that of HBO and compound 3, implying insufficient proton transfer. Different from HBO and compounds 2-3, ESIPT of compound 1 is endothermic and the energy of keto (S_1) is 2.6 kcal/mol higher than that of enol (S_1) . Besides, the energy barrier is also very high (3.6 kcal/mol) compared with the other compounds examined here. The two facts rationalize the prohibition of ESIPT for compound 1. Therefore, the TD-DFT results are consistent with our observations in the fs-TA and ns-TA results, which provides further evidence for the assignments in this work.

We plotted the fluorescence area ratio of keto to enol emission $(R_{\rm k/e})$ versus the computed energy difference (ΔE^*) (Figure S15) and perceived a trend that the smaller ΔE^* lead to a larger $R_{\rm k/e}$. As ΔE^* and the equilibrium constant (K) have a negative correlation with each other (based on the formula $\Delta G = -RT \ln K$), $R_{\rm k/e}$ can be roughly used to represent the equilibrium constant of the ESIPT reaction in the ESIPT systems with small energy barriers. To be specific, the larger the ratio is, the more thorough the ESIPT is, and the smaller this ratio is the more severe the ESIPT is suppressed.

For all of these compounds, the computed lowest-lying electronic transition $(S_0 \rightarrow S_1)$ in terms of the wavelength agrees well with the experimental results (Table 1), supporting the validity of the current computational approach. We first optimized the structures of all the compounds at So and Si state for more details. At the ground state, the dihedral angles $(\varphi, \text{ Table S1})$ between the benzoxazole moiety and the substituent segment with the hydroxyl group for HBO and compounds 1, 2 are close to 0°, which indicates that these three compounds take a coplanar geometry and thus ensure a full π -conjugation between the two units. However, the φ value for compound 3 is noticeably larger (14.047°), implying that compound 3 has less efficient conjugation. The O₁-H₁ and N_1 - H_1 bond distances for the titled compounds are calculated and summarized in Table S1. After excitation to the S1 state, the O₁-H₁ bond lengths increase and those for the N₁-H₁ bonds decrease for all of the four compounds, which suggest that the intramolecular hydrogen bond strength is enhanced after excitation. However, for the different compounds, the variation percentage of the N₁-H₁ or O₁-H₁ bond lengths are different. For example, the N₁-H₁ bond length of HBO is reduced from 1.78152 to 1.71411 Å and the change percentage is 3.78%. Both the O_1-H_1 (0.09%) and N_1-H_1 (0.24%) bond length variations of compound 1 are negligible, indicating ESIPT of compound 1 is not as strongly favored as that of HBO, which is in good agreement with the experimentally observed prohibition of ESIPT for compound 1.

The highest occupied molecular orbitals (HOMO) and lowest unoccupied molecular orbitals (LUMO) for HBO and compounds 1-3 are listed in Table 2. For HBO, the HOMO and LUMO spread over the whole molecular skeleton and the overall charge-transfer character in the transition is not significant. Whereas the electron density on the O atom of the hydroxyl group decreases and the electron density on the N_1 atom of the benzoxazole moiety increases from HOMO to LUMO, which indicates that both the acidity of the hydroxyl group and the basicity of the N_1 atom are enhanced upon photoexcitation, promoting ESIPT from a dynamical point of view. Thus, the shift of the electron density from the O_1 atoms to the N_1 atom serves as a driving force for ESIPT. It should be noted the electron density of the N_1 atom is much larger than that of the O_1 atom for HBO's LUMO.

Different from **HBO**, for compound 3 the electron density population of the HOMO spreads all over the molecule while its LUMO appears mainly distributed on the **HBO** unit and one benzene ring of phenanthrene which is closer to the hydroxyl group. Such an electron density change after the transition from HOMO \rightarrow LUMO suggests that the S₁ state of

Table 2. Computed Frontier Orbitals for HBO and Compounds 1-3 in Their Enol Form Involved in the First Singlet Excitation at the Optimized Ground State Geometries^a

Compound	нво	3	2	1
LUMO				
номо				

^aThe calculations were performed at the wB97XD/def2tzvp (DCM) level of theory (contour value, 0.036).

compound 3 has a typical intramolecular charge transfer (ICT) character. Additionally, the electron density of the O_1 atom of the hydroxyl group decreases a little while the N heteroatom in the **HBO** segment keeps almost unchanged after excitation. Besides, the electron density of N_1 is only a little higher than that of O_1 in compound 3's LUMO, which validates the insignificant driving force of ESIPT in this case.

With the introduction of the strong electron-withdrawing thiadiazol and pyrazine groups in compounds 1 and 2, their HOMOs are mainly located on the HBO unit, and their LUMO shifts to the electron-withdrawing group containing the terminal part of both molecules, leading to significant ICT. For compound 1, after being excited to the S₁ state another noticeable character is the reduction of the electron density surrounding the N atom of the benzoxazole groups, weakening the attraction between the N and H atoms and the intramolecular hydrogen bonds, thus the energy barrier for the proton transfer is large (Figure S14) and ESIPT is not efficient or even prohibited when the barrier is high enough. Similar to compound 1, the electron density on the N₁ atom reduces significantly upon excitation but the energy barrier for the proton transfer is smaller for compound 2 than that of compound 1 (Figure S14). This is because the electronwithdrawing ability of pyrazine is weaker compared with thiadiazol. The electron density of the O_1 and N_1 atoms looks the same for compound 1's LUMO, which may be responsible for the lack of ESIPT of compound 1.

CONCLUSIONS

A series of novel compounds 1-3 based on the HBO unit were synthesized. The steady-state absorption/emission and time-resolved absorption spectroscopic experiments as well as DFT/TD-DFT calculations were employed to investigate the photophysical properties and photochemical reaction mechanisms of HBO and compounds 1-3. Analogue non-ESIPT molecules Me1-Me3 have also been studied for comparison purposes. Compounds 1-3 have a larger π -conjugation framework and display red-shifted absorbance compared with HBO. Among the four compounds, HBO shows an ultrafast ESIPT while compound 3 has an equilibrium type of ESIPT

with dual emission. The absence of the keto fluorescence in compounds 1 and 2 indicates there is a significant influence of the electron-withdrawing group on the ESIPT properties. It is found that the introduction of an electron-withdrawing segment such as thiadiazol and pyrazine in the hydroxyphenyl ring (compounds 1 and 2) apparently suppresses the proton-transfer in the excited states. Our findings reported herein are valuable to develop a more thorough understanding of structure—property relationships of ESIPT molecules and will hopefully inspire more research into this intriguing area.

ASSOCIATED CONTENT

Supporting Information

are shown in Supporting Information. The Supporting Information is available free of charge at https://pubs.acs.org/doi/10.1021/acs.jpcb.1c05798.

The experimental setup of fs-TA, ns-TA, the synthetic details and characterization of 1–3 and Me1–Me3, the steady state absorption and emission spectra of HBO and 1–3, ns-TA spectra of HBO and 1–3, fs-TA spectra of Me1–Me3, potential energy profiles and calculation results and optimized coordinates of HBO and 1–3 (PDF)

AUTHOR INFORMATION

Corresponding Authors

Lili Du — School of Life Sciences, Jiangsu University, Zhenjiang 212013, P.R. China; Department of Chemistry, The University of Hong Kong, Hong Kong, Hong Kong, S.A.R., P.R. China; orcid.org/0000-0002-9712-3925; Email: dulili@ujs.edu.cn

David Lee Phillips — Department of Chemistry, The University of Hong Kong, Hong Kong, Hong Kong, S.A.R., P.R. China; orcid.org/0000-0002-8606-8780; Email: phillips@hku.hk

Authors

Yuanchun Li — School of Life Sciences, Jiangsu University, Zhenjiang 212013, P.R. China; Department of Chemistry, The University of Hong Kong, Hong Kong, Hong Kong, S.A.R., P.R. China

 Xueqin Bai — Department of Chemistry, The University of Hong Kong, Hong Kong, Hong Kong, S.A.R., P.R. China
 Runhui Liang — Department of Chemistry, The University of Hong Kong, Hong Kong, Hong Kong, S.A.R., P.R. China

Xiting Zhang — Department of Chemistry, The University of Hong Kong, Hong Kong, Hong Kong, S.A.R., P.R. China; orcid.org/0000-0001-7602-1965

Yen H. Nguyen – Department of Chemistry, Iowa State University, Ames, Iowa 50011, United States

Brett VanVeller — Department of Chemistry, Iowa State University, Ames, Iowa 50011, United States; ⊚ orcid.org/ 0000-0002-3792-0308

Complete contact information is available at: https://pubs.acs.org/10.1021/acs.jpcb.1c05798

Author Contributions

"Y.L. and X.B. contributed equally to this work.

Notes

The authors declare no competing financial interest.

ACKNOWLEDGMENTS

This work was supported by grants from the National Science Fund of China (21803026) and Natural Science Foundation of Jiangsu Province (BK20180854), the Hong Kong Research Grants Council (GRF 17302419), The University of Hong Kong Development Fund 2013-2014 project "New Ultrafast Spectroscopy Experiments for Shared Facilities" and Seed Fund for Basic Research Grant 202011159051, Major Program of Guangdong Basic and Applied Research (2019B030302009), and Guangdong-Hong Kong-Macao Joint Laboratory of Optoelectronic and Magnetic Functional Materials (2019B121205002). B.V. and Y.H.N. acknowledge the National Science Foundation, Division of Chemistry (grant no. 1848261).

REFERENCES

- (1) Abou-Zied, O. K.; Jimenez, R.; Thompson, E. H.; Millar, D. P.; Romesberg, F. E. Solvent-dependent photoinduced tautomerization of 2-(2'-hydroxyphenyl) benzoxazole. *J. Phys. Chem. A* **2002**, *106*, 3665—3672.
- (2) Guest, C. R.; Hochstrasser, R. A.; Allen, D. J.; Benkovic, S. J.; Millar, D. P.; Dupuy, C. G. Interaction of DNA with the Klenow fragment of DNA polymerase I studied by time-resolved fluorescence spectroscopy. *Biochemistry* **1991**, *30*, 8759–8770.
- (3) Iijima, T.; Momotake, A.; Shinohara, Y.; Sato, T.; Nishimura, Y.; Arai, T. Excited-state intramolecular proton transfer of naphthalene-fused 2-(2'-hydroxyaryl) benzazole family. *J. Phys. Chem. A* **2010**, *114*, 1603–160.
- (4) Massue, J.; Jacquemin, D.; Ulrich, G. Molecular engineering of excited-state intramolecular proton transfer (ESIPT) dual and triple emitters. *Chem. Lett.* **2018**, 47, 1083–1089.
- (5) Papadakis, R.; Ottosson, H. The excited state antiaromatic benzene ring: a molecular Mr Hyde? *Chem. Soc. Rev.* **2015**, *44*, 6472–6493.
- (6) Heller, A.; Williams, D. L. Intramolecular proton transfer reactions in excited fluorescent compounds. *J. Phys. Chem.* **1970**, *74*, 4473–4480.
- (7) Wu, J.; Liu, W.; Ge, J.; Zhang, H.; Wang, P. New sensing mechanisms for design of fluorescent chemosensors emerging in recent years. *Chem. Soc. Rev.* **2011**, *40*, 3483–3495.
- (8) Zhao, J.; Ji, S.; Chen, Y.; Guo, H.; Yang, P. Excited state intramolecular proton transfer (ESIPT): from principal photophysics to the development of new chromophores and applications in fluorescent molecular probes and luminescent materials. *Phys. Chem. Chem. Phys.* **2012**, *14*, 8803–8817.
- (9) Tomin, V. I.; Demchenko, A. P.; Chou, P.-T. Thermodynamic vs. kinetic control of excited-state proton transfer reactions. *J. Photochem. Photobiol., C* **2015**, 22, 1–18.
- (10) Weller, A. Innermolekularer protonenübergang im angeregten zustand. Z. Elektrochem. 1956, 60, 1144–1147.
- (11) D'Andrade, B. W.; Holmes, R. J.; Forrest, S. R. Efficient organic electrophosphorescent white-light-emitting device with a triple doped emissive layer. *Adv. Mater.* **2004**, *16*, 624–628.
- (12) Kim, T. H.; Lee, H. K.; Park, O. O.; Chin, B. D.; Lee, S. H.; Kim, J. K. White-Light-Emitting Diodes Based on Iridium Complexes via Efficient Energy Transfer from a Conjugated Polymer. *Adv. Funct. Mater.* **2006**, *16*, 611–617.
- (13) Kim, S.; Park, S. Y. Photochemically gated protonation effected by intramolecular hydrogen bonding: towards stable fluorescence imaging in polymer films. *Adv. Mater.* **2003**, *15*, 1341–1344.
- (14) Sobolewski, A. L.; Domcke, W. Photophysics of intramolecularly hydrogen-bonded aromatic systems: ab initio exploration of the excited-state deactivation mechanisms of salicylic acid. *Phys. Chem. Phys.* **2006**, *8*, 3410–3417.
- (15) Parthenopoulos, D. A.; McMorrow, D. P.; Kasha, M. Comparative study of stimulated proton-transfer luminescence of three chromones. *J. Phys. Chem.* **1991**, *95*, 2668–2674.

- (16) Mohammed, O. F.; Pines, D.; Nibbering, E. T.; Pines, E. Base-Induced Solvent Switches in Acid—Base Reactions. *Angew. Chem.* **2007**, *119*, 1480—1483.
- (17) Park, S.; Kwon, O.-H.; Kim, S.; Park, S.; Choi, M.-G.; Cha, M.; Park, S. Y.; Jang, D.-J. Imidazole-based excited-state intramolecular proton-transfer materials: synthesis and amplified spontaneous emission from a large single crystal. *J. Am. Chem. Soc.* **2005**, *127*, 10070–10074.
- (18) Lim, S.-J.; Seo, J.; Park, S. Y. Photochromic switching of excited-state intramolecular proton-transfer (ESIPT) fluorescence: a unique route to high-contrast memory switching and nondestructive readout. J. Am. Chem. Soc. 2006, 128, 14542–14547.
- (19) Nunes, R. M.; Pineiro, M.; Arnaut, L. G. Photoacid for extremely long-lived and reversible pH-jumps. *J. Am. Chem. Soc.* **2009**, 131, 9456–9462.
- (20) Kanda, T.; Momotake, A.; Shinohara, Y.; Sato, T.; Nishimura, Y.; Arai, T. Photoinduced Proton Transfer in 2-(2'-Hydroxynaphthalenyl) benzoxazole: Observation of Fluorescence with a Small Stokes Shift Induced by Excited-State Intramolecular Proton Transfer. *Bull. Chem. Soc. Jpn.* **2009**, 82, 118–120.
- (21) Liu, Z.-Y.; Hu, J.-W.; Chen, C.-L.; Chen, Y.-A.; Chen, K.-Y.; Chou, P.-T. Correlation among Hydrogen Bond, Excited-State Intramolecular Proton-Transfer Kinetics and Thermodynamics for—OH Type Proton-Donor Molecules. *J. Phys. Chem. C* **2018**, *122*, 21833—21840.
- (22) Mutai, T.; Sawatani, H.; Shida, T.; Shono, H.; Araki, K. Tuning of excited-state intramolecular proton transfer (ESIPT) fluorescence of imidazo [1, 2-a] pyridine in rigid matrices by substitution effect. *J. Org. Chem.* **2013**, *78*, 2482–2489.
- (23) Chen, C.-L.; Chen, Y.-T.; Demchenko, A. P.; Chou, P.-T. Amino proton donors in excited-state intramolecular proton-transfer reactions. *Nat. Rev. Chem.* **2018**, *2*, 131–143.
- (24) Azarias, C.; Budzák, Š.; Laurent, A. D.; Ulrich, G.; Jacquemin, D. Tuning ESIPT fluorophores into dual emitters. *Chem. Sci.* **2016**, *7*, 3763–3774.
- (25) Ma, J.; Zhao, J.; Yang, P.; Huang, D.; Zhang, C.; Li, Q. New excited state intramolecular proton transfer (ESIPT) dyes based on naphthalimide and observation of long-lived triplet excited states. *Chem. Commun.* **2012**, *48*, 9720–9722.
- (26) Gupta, A. K.; Kumar, A.; Singh, R.; Devi, M.; Dhir, A.; Pradeep, C. Facile synthesis of an organic solid state near-infrared-emitter with large Stokes shift via excited-state intramolecular proton transfer. *ACS Omega.* **2018**, *3*, 14341–14348.
- (27) Antonov, L.; Nedeltcheva, D. Resolution of overlapping UV–Vis absorption bands and quantitative analysis. *Chem. Soc. Rev.* **2000**, 29, 217–227.
- (28) Nedeltcheva, D.; Antonov, L.; Lycka, A.; Damyanova, B.; Popov, S. Chemometric models for quantitative analysis of tautomeric Schiff bases and azo dyes. *Curr. Org. Chem.* **2009**, *13*, 217–240.
- (29) Antonov, L. Absorption UV-Vis spectroscopy and chemometrics: from qualitative conclusions to quantitative analysis. *Tautomerism: methods and theories* **2013**, 25–47.
- (30) Hsieh, C.-C.; Chou, P.-T.; Shih, C.-W.; Chuang, W.-T.; Chung, M.-W.; Lee, J.; Joo, T. Comprehensive studies on an overall proton transfer cycle of the ortho-green fluorescent protein chromophore. *J. Am. Chem. Soc.* **2011**, *133*, 2932–2943.
- (31) Dahal, D.; McDonald, L.; Bi, X.; Abeywickrama, C.; Gombedza, F.; Konopka, M.; Paruchuri, S.; Pang, Y. An NIR-emitting lysosometargeting probe with large Stokes shift via coupling cyanine and excited-state intramolecular proton transfer. *Chem. Commun.* **2017**, *53*, 3697–3700.
- (32) Chung, M.-W.; Lin, T.-Y.; Hsieh, C.-C.; Tang, K.-C.; Fu, H.; Chou, P.-T.; Yang, S.-H.; Chi, Y. Excited-state intramolecular proton transfer (ESIPT) fine tuned by quinoline—pyrazole isomerism: π -conjugation effect on ESIPT. *J. Phys. Chem. A* **2010**, *114*, 7886–7891.
- (33) Massue, J.; Felouat, A.; Vérité, P. M.; Jacquemin, D.; Cyprych, K.; Durko, M.; Sznitko, L.; Mysliwiec, J.; Ulrich, G. An extended excited-state intramolecular proton transfer (ESIPT) emitter for

- random lasing applications. Phys. Chem. Chem. Phys. 2018, 20, 19958–19963.
- (34) Brewer, W. E.; Martinez, M. L.; Chou, P. T. Mechanism of the ground-state reverse proton transfer of 2-(2-hydroxyphenyl) benzothiazole. *J. Phys. Chem.* **1990**, *94*, 1915–1918.
- (35) Al-Soufi, W.; Grellmann, K. H.; Nickel, B. Triplet state formation and cis→ trans isomerization in the excited singlet state of the keto tautomer of 2-(2'-hydroxyphenyl) benzothiazole. *Chem. Phys. Lett.* **1990**, *174*, 609−616.
- (36) Chou, P.-T.; Martinez, M. L.; Studer, S. L. The role of the cisketo triplet state in the proton transfer cycle of 2-(2'-hydroxyphenyl) benzothiazole. *Chem. Phys. Lett.* **1992**, *195*, 586–590.
- (37) Stephan, J. S.; Rodríguez, C. R.; Grellmann, K. H.; Zachariasse, K. A. Flash-photolysis of 2-(2'-hydroxyphenyl)-3-H-indole. Ground-state keto-enol tautomerization by mutual hydrogen exchange and by proton catalysis. *Chem. Phys.* **1994**, *186*, 435–446.
- (38) Stephan, J. S.; Grellmann, K. H. Photoisomerization of 2-(2'-Hydroxyphenyl) benzoxazole. Formation and Decay of the Trans-Keto Tautomer in Dry and in Water-Containing 3-Methylpentane. *J. Phys. Chem.* **1995**, *99*, 10066–10068.